JANUSZ LELITO, PAWEŁ ŻAK, JÓZEF SUCHY, WITOLD KRAJEWSKI, HALINA KRAWIEC, LINDSAY GREER, PETER SCHUMACHER, AMIR SHIRZADI, KATHARINA HABER, PAWEŁ DARŁAK

Modelling the effect of SiC mass fraction on crystallization of magnesium metal matrix composite; AZ91/SiC

INTRODUCTION

Grain size is one of the most important parameter which determined mechanical properties. Knowing element properties the proper application regions for it can be chosen to achieve best mechanical properties and performance. Nowadays simulation software can be use to predict the element microstructure. Those programs base on micro-macro model of crystallization. The model consists of partial differential equations (PDEs) that described the nucleation rate, diffusion in the casting, casting cooling speed and every single grain growth rate. Often it is hard to find the theoretical value of the parameters that appear in those PDEs. It is possible to find them from experiment. The experimental data that after applying statistical methods let us find approximated values of the so-called "fitting parameters" in the mentioned models [1÷4].

AZ91 alloy analyzed in this study is hypereutectic alloy. The magnesium primary α-Mg phase is dendritic. During crystallisation there appears eutectic reaction. In this study influence of eutectic is omitted because magnesium primary phase has most significant influence on mechanical properties of the casting.

EXPERIMENTAL PROCEDURE

Composite casting

The AZ91 alloy was selected as the matrix for the composites. The chemical composition is shown in Table 1. The reinforcement particles are silicon carbide with an average diameter of 45 μm. Composite specimen with 0, 1, 2, 3 and 4 wt. % of SiC particles were prepared using a liquid mixing and casting process.

Processing of the magnesium composites consisted of mixing pre-heated SiC particles to 450°C with liquid magnesium melt stirring and mould casting. About 1.4 kg of composite melts was prepared in an electric resistance furnace using a steel crucible under a SF_6/CO_2 gas atmosphere. The molten AZ91 alloy was held at 700°C for 1 h. After putting SiC particles composite was stirred for 2 min, and then cast at 700°C into mould to produce four plates of 100×100×10 (plate no. 1), 15 (plate no. 2), 20 (plate no. 3) and 30 mm (plate no. 4) – Figure 1. The mould was made with resin sand hardened with CO_2. An un-reinforced AZ91 alloy was also cast at the same temperature (700°C).

Table 1. Chemical composition of AZ91 alloy
Tabela 1. Skład chemiczny stopu AZ91

Chemical composition, wt. %							
Al	Zn	Mn	Fe	Be	Si	Cu	Ni
9.03	0.6	0.2	0.0026	0.0011	0.0023	0.0016	0.00062

Thermal analysis

For the thermal analysis of AZ91 alloy and composite samples, cooling curves during solidification were obtained using a data acquisition system (Agilent) at a sampling rate of 5 data per second. A chromel-alumel (K-type) thermocouple positioned 50 mm from the bottom of the plate center, was used to monitoring temperature as the melt solidified.

Microstructural analysis and grain size determination

The as-cast plates were sectioned at a distance 3 mm from hot junction of a thermocouple and next polished and etched before microstructural analysis. In order to visualization of grain boundaries of magnesium primary phase, the metallographic specimens were etched for 80÷95 s. The chemical composition of solution was: 50 ml distilled water, 150 ml ethanol, 1 ml acetic acid [5÷7].

The etched specimens were examined using a light microscope Carl Zeiss AXIO Imager.A1 with cross polarized light and λ filter. The grains density was counted on the surface of etched specimens using image analysis NIS-Elements 3.0 Software. The images on computer display reveal arms of different dendrite grains as areas with different colours (Fig. 2).

NUMERICAL MODEL

Numerical micro-macro model of AZ91/SiC composite solidification is base on differential equations heat and mass transport.

We assume, that the heat condition process play main role in heat transport and therefore temperature field can be described by the Fourier-Kirchhoff equations:

$$\frac{\partial T}{\partial \tau} = a\nabla^2 T + \frac{q_v}{c_v}, \text{ K/s} \quad (1)$$

where: T – temperature, K, τ – time, s, a – heat of diffusivity coefficient, m^2s^{-1}, q_v – heat of crystallization, Wm^{-3}, c_v – specific heat, $Jm^{-3}K^{-1}$.

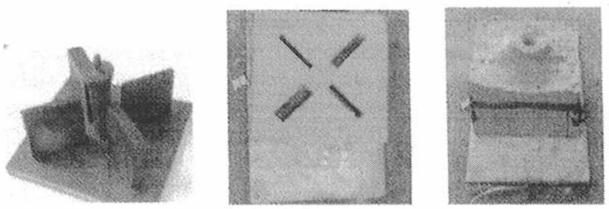

Fig. 1. Photo of gating system with four plates (a) and synthetic resin sand hardened with CO_2 mould (b, c)
Rys. 1. Zdjęcia układu wlewowego z czteroma płytkami (a) i formy odlewniczej na bazie piasku kwarcowego z żywicą syntetyczną utwardzaną CO_2 (b, c)

Ph.D. **Janusz Lelito** (lelito@agh.edu.pl), M.Sc. **Paweł Żak**, Prof. **Józef Suchy**, Prof. **Witold Krajewski**, Ph.D. **Halina Krawiec** – AGH University of Science and Technology, PL, Prof. **Lindsay Greer** – Department of Materials Science and Metallurgy, University of Cambridge, UK, Ph.D. **Amir Shirzadi** – Materials Engineering, The Open University, UK and Department of Materials Science and Metallurgy, University of Cambridge, UK, Prof. **Peter Schumacher**, M.Sc. **Katharina Haber** – Department of Metallurgy, University of Leoben, AT, M.Sc. **Paweł Darłak** – Foundry Research Institute in Krakow, PL

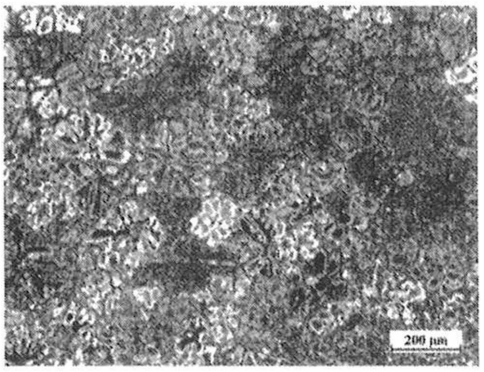

Fig. 2. Example of microstructure of AZ91/SiC composite for sample was cut from as-cast plate about thickness 10 mm with 2 wt. % of SiC
Rys. 2. Przykładowe zdjęcie mikrostruktury płytki o grubości 10 mm dla kompozytu AZ91/SiC z 2% mas. SiC

The crystallization heat is defined as follows:

$$q_V = L\frac{\partial f_s}{\partial \tau} \tag{2}$$

where: L – latent heat of magnesium primary phase crystallization, Jm^{-3}, f_s – solid state fraction of magnesium primary phase.

Solid state fraction was calculated from equation:

$$f_s = \sum_{n=1}^{n} \frac{4}{3}\pi R_i^3 N_i \tag{3}$$

where: N_i – grains density in i-class, m^{-3}, R_i – grain radius in i-class, m.

After rearranged above an equation was obtained solid state growth rate equation:

$$\frac{\partial f_s}{\partial \tau} = \sum_{i=1}^{n} 4\pi R_i^2 N_i \frac{\partial R_i}{\partial \tau} \tag{4}$$

where: $\frac{\partial R}{\partial \tau}$ – grain growth rate, ms^{-1}.

During the nucleation processes new grains appear ($N_{n+1} = \frac{\partial N_V}{\partial \tau}$) which have essential influence on solid state function. This process is described by equation:

$$f_s = f_s + \frac{4}{3}\pi R_{n+1}^3 N_{n+1} \tag{5}$$

After normal grain growth stage is taken into account with solid state growth rate (4).

In order to calculate grain growth rate they have to couple above model with diffusion-kinetic model of composite solidification.

The spherical growth model is assumed to describe magnesium primary phase formation. This process is controlled by aluminum diffusion coupled with temperature field. Diffusion aluminum proceeds between sphere of primary phase (α-Mg) and surrounded liquid. Second Fick's law and mass balance describe interface moving between primary phase (α-Mg) and surrounded liquid. In the cylindrical coordinate system kinetic of aluminum concentration is described by equation:

– for magnesium primary phase (α-Mg):

$$\frac{dC}{d\tau} = D_\alpha\left(\frac{\partial^2 C}{\partial r^2} + \frac{2}{r}\frac{\partial C}{\partial r}\right) + \frac{r}{R}\frac{\partial C}{\partial r}\frac{dR}{d\tau} \tag{6}$$

– for liquid:

$$\frac{dC}{d\tau} = D_L\left(\frac{\partial^2 C}{\partial r^2} + \frac{2}{r}\frac{\partial C}{\partial r}\right) + \frac{R_o - r}{R_o - R}\frac{\partial C}{\partial r}\frac{dR}{d\tau} \tag{7}$$

where: C_L – Al liquidus concentration for actual temperature, C_S – Al solidus concentration for actual temperature, r – distance from the grain center, m, R – interface distance from the grain center, m, R_o – maximal possible radius, m.

Considering the interface, equations (6) and (7) are related with the mass balance equation (8).

Mass balance at the primary phase (α-Mg) – phase liquid interface:

$$(C_L - C_S)\frac{dR}{d\tau} = D_{Al}^{\alpha}\frac{dC_\alpha}{dR}\bigg|_{R^-} - D_{Al}^{L}\frac{dC_L}{dR}\bigg|_{R^+} \tag{8}$$

where: D_{Al}^{α}, D_{Al}^{L} – diffusion coefficient of aluminium in magnesium primary phase and in liquid, m^2s^{-1}.

Above equations (6÷8) are analogous to those presented in [8, 9].

The maximal radius was calculated for all grains-class:

$$R_o = \sqrt[3]{\frac{3(1-V)}{4\pi}} \tag{9}$$

This situation have place when every one of grain try to consume rest liquid volume.

Solution of above an equation system gives interface moving rate.

Grain density

Data obtained from metallographic analysis can be used to calculate the grain's density per unit volume, N_V. To find this value Saltykov equation can be used [10]:

$$N_V = \frac{2}{\pi}\cdot N_a \cdot \left(\frac{1}{d}\right)_{mean},\ m^{-3} \tag{10}$$

where: N_V is mean the grain's density per unit volume, N_a is mean surface grain density, and $\left(\frac{1}{d}\right)_{mean}$ denotes average value of $\left(\frac{1}{d}\right)$ for all grains found on the polished section.

In this article the continuous nucleation model is taking into account. It is based on log-normal model described by Fras et al. in [4]:

$$N_V = \lambda \cdot \exp\left(-\frac{b}{\Delta T_{max}}\right),\ m^{-3} \tag{11}$$

where: λ, m^{-3}, b, K – are model adjustment parameters, that should be find experimentally and ΔT_{max} denotes maximal undercooling.

It was shown by various authors that character of continuous nucleation [11, 12] is similar to model presented by Fras. According to this fact, as nucleation and crystallization simulation is performed, calculation of N_V step by step changes is connected with time by actual undercooling, denoted ΔT. During this calculation eq. (11) is used but for actual ΔT in the place of maximal undercooling ΔT_{max}.

Partial differential Fourier-Kirchhoff equation solved in parallel gives the actual $\Delta T(\tau) = T_N - T(\tau)$, where τ is time. The different maximal undercoolings, measured during the castings and connected volumetric grain densities gives us test values to calculate fitting parameters in equation (11). More complex model can be obtained if one use experimental data for different mass fraction of SiC particles, denoted mf_{SiC}. The test values can be than used to find functions that describes λ and b parameters dependence on the mass fraction of SiC particles. The model that takes into account those functions can be expressed with formula:

$$N_V(\Delta T) = \lambda(mf_{SiC}) \cdot \exp\left(-\frac{b(mf_{SiC})}{\Delta T}\right),\ m^{-3} \tag{12}$$

The another parameter that is necessary for modeling of composite nucleation and crystallization is nucleation temperature, T_N. This value for composites depends on the mass fraction of SiC particles [2]. It also can be expressed with proper formula that can be finding statistically. Nucleation temperature can be obtained from thermoa-

nalysis data, precisely from first derivative of cooling curve analysis, according to the procedure described by Kurz and Fisher [13].

RESULTS

Grain density of magnesium primary phase

The equilibrium phase for AZ91/SiC composite is the solid α-Mg solution, but during solidification a nonequilibrium eutectic (α-Mg $-\beta$-$Mg_{17}Al_{12}$) is also created and present in the un-reinforced AZ91 alloy and in the AZ91/SiC composite.

From thermoanalysis cooling curves the nucleation temperature, T_N, and maximal undercooling of primary phase, ΔT_{max}, can be calculated as a difference between nucleation and recalescence temperature. There are obtain from cooling curve and its first derivative. The nucleation temperature grows with increasing mass fraction of the SiC particles. The exponential dependence can be observed, it can be described with fallowing formula:

$$T_N\left(mf_{SiC}\right) = 606 - 5.8\exp\left(-90.4mf_{SiC}\right) \quad , °C \qquad (13)$$

where: mf_{SiC} denotes dimensionless mass fraction of SiC particles in the composite.

The above formula was calculated, correlation coefficient for this fitting was $R^2 = 0.991$. The graph of statistically evaluated curve (13) is shown in Figure 3.

Average grain diameter measurement data can be used also to calculate average volumetric grain density. This parameter is widely used to describe casting refinement of structure. It also is very useful during simulation, because it carries information about number of nuclei appearing in the unit of volume. The mean grain's density per unit volume, N_V, was calculated from Saltykov equation (10).

The grain's density N_V and corresponding maximal undercooling ΔT_{max} were used as the test values for approximate the adjustment parameters in Fras equation (11). For mass fraction of SiC particles the calculated equations have the following form:

– for 0 wt. % SiC, $R^2 = 0.999$ (Fig. 4:

$$N_V = 1184 \cdot 10^9 \exp\left(-\frac{27.354}{\Delta T_{max}}\right) \quad , m^{-3} \qquad (14)$$

– for 1 wt. % SiC, $R^2 = 0.989$ (Fig. 5):

$$N_V = 5778 \cdot 10^9 \exp\left(-\frac{29.95}{\Delta T_{max}}\right) \quad , m^{-3} \qquad (15)$$

– for 2 wt. % SiC, $R^2 = 0.993$ (Fig. 6):

$$N_V = 5815 \cdot 10^{10} \exp\left(-\frac{85.9}{\Delta T_{max}}\right) \quad , m^{-3} \qquad (16)$$

– for 3 wt. % SiC, $R^2 = 0.997$ (Fig. 7):

$$N_V = 1071 \cdot 10^{11} \exp\left(-\frac{102.26}{\Delta T_{max}}\right) \quad , m^{-3} \qquad (17)$$

– for 4 wt. % SiC, $R^2 = 0.996$ (Fig. 8):

$$N_V = 1619 \cdot 10^{11} \exp\left(-\frac{104.85}{\Delta T_{max}}\right) \quad , m^{-3}. \qquad (18)$$

The presented formulas can be used to describe the grain density function for specific mass fraction of SiC particles. Moreover if the maximal undercooling ΔT_{max} is replaced with actual under-cooling ΔT the presented equations can be use for continuous nucleation problem.

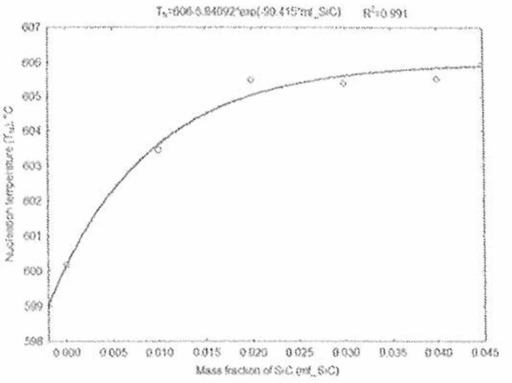

Fig. 3. The nucleation temperature dependence on mass fraction of SiC particles

Rys. 3. Temperatura zarodkowania zależna od udziału masowego cząstek SiC

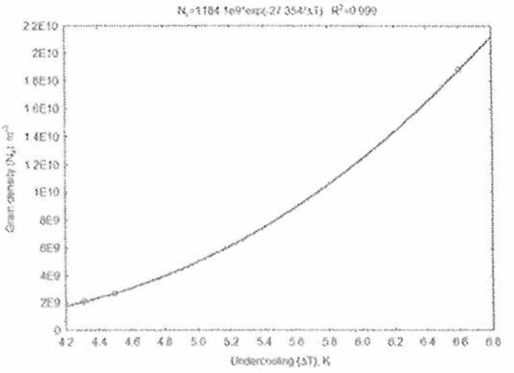

Fig. 4. The grain density dependence on undercooling for AZ91/0 wt. % SiC composite

Rys. 4. Zależność gęstości ziaren od przechłodzenia dla kompozytu AZ91/SiC z 0% mas. SiC

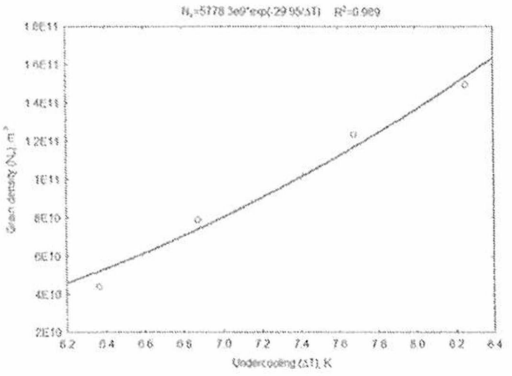

Fig. 5. The grain density dependence on undercooling for AZ91/1 wt. % SiC composite

Rys. 5. Zależność gęstości ziaren od przechłodzenia dla kompozytu AZ91/SiC z 1% mas. SiC

Further analysis of the experimental data leads to more general conclusion, that is, model for continuous nucleation that takes into account grain size. It can be described with the following expression:

$$N_V\left(\Delta T, mf_{SiC}\right) = 1.42 \cdot 10^{13} \exp\left(61.9 \cdot mf_{SiC} - \frac{36.25 \cdot \exp\left(29.3 \cdot mf_{SiC}\right)}{\Delta T}\right), m^{-3} \qquad (19)$$

The correlation coefficient for this equation is $R^2 = 0.866$. Equation (19) can be used during nucleation simulation of the AZ91/SiC composites with different mass fraction of reinforcement particles.

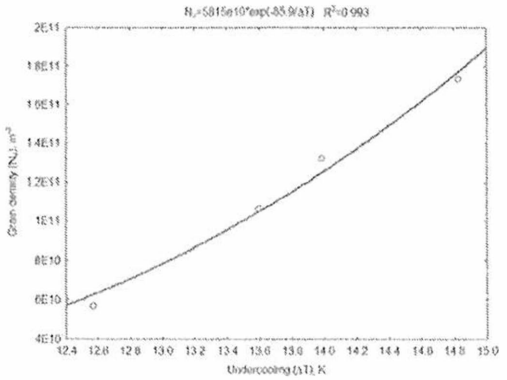

Fig. 6. The grain density dependence on undercooling for AZ91/2 wt. % SiC composite
Rys. 6. Zależność gęstości ziaren od przechłodzenia dla kompozytu AZ91/SiC z 2% mas. SiC

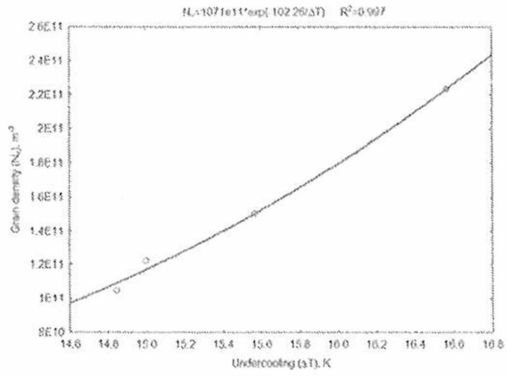

Fig. 7. The grain density dependence on undercooling for AZ91/3 wt. % SiC composite
Rys. 7. Zależność gęstości ziaren od przechłodzenia dla kompozytu AZ91/SiC z 3% mas. SiC

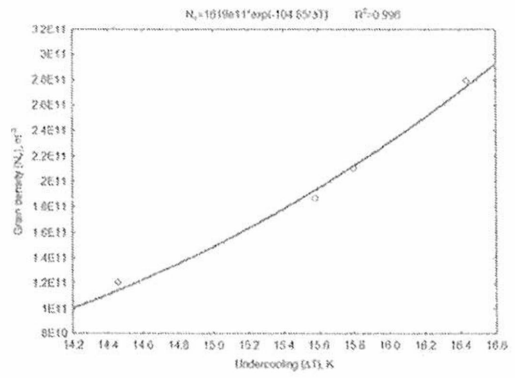

Fig. 8. The grain density dependence on undercooling for AZ91/4 wt. % SiC composite
Rys. 8. Zależność gęstości ziaren od przechłodzenia dla kompozytu AZ91/SiC z 4% mas. SiC

Figure 9 shows how the average volumetric grain density N_V, depends on undercooling and mass fraction of SiC particles. It can be seen that with the undercooling growth the grain density grows very rapidly. This effect is greater for the smaller mass fraction of SiC particles.

The formula presented above gives possibility to calculate grain density continuously while melt temperature decreasing.

The nucleation model linked with the FK solving numerical scheme can be used to obtain very good approximation of the composite cooling speed, forming of the solid stage rate and to predict its microstructure.

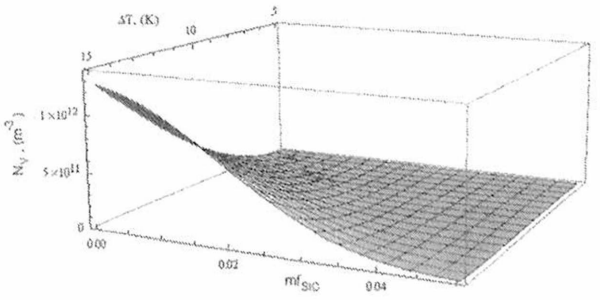

Fig. 9. 3-D representation of N_V dependence on alloy undercooling and mass fraction of SiC particles (dimensionless)
Rys. 9. 3-W wykres zależności N_V od przechłodzenia stopu i udziału masowego cząstek SiC (bezwymiarowy)

Because of the lack of theoretical data, results of numerical analysis of composite nucleation phenomena (equations (14)÷(19) presented above) can be very useful. Those equations linked with FK equation can give a lot of important information about AZ91/SiC composite crystallization phenomena.

Numerical simulation

For the numerical simulation we assumed initial data:

a) diffusion coefficient: : $D_{Al}^{\alpha} = 2.7 \cdot 10^{-10}$ m^{2}s^{-1}, $D_{Al}^{L} = 2.7 \cdot 10^{-8}$ m^{2}s^{-1},
b) nucleation temperature is describe by equation (13) (for 5 wt. % of SiC),
c) initial temperature is 700°C,
d) grain density is describe by equation (19) (for $d_{SiC} = 45$ μm),
e) parameter $\zeta_V^L = 267.86$ K,
f) we assumed cooling rate ($P = a\nabla^2 T$) depend on temperature and connected with material of mould:

$$P(T) = \begin{cases} -40 & \text{for } T > 625^{\circ}C, \\ \frac{200}{T-630} & \text{for } 625^{\circ}C \geq T > 620^{\circ}C, \\ \frac{5T-2900}{T-630} & \text{for } 620^{\circ}C \geq T > 600^{\circ}C, \\ \frac{100}{T-630} & \text{for } T \leq 600^{\circ}C. \end{cases} \tag{20}$$

Results of the simulation were later validated with experimental casting. The simulation run for AZ91/SiC composite of 5% content of SiC, $d_{SiC} = 45$ μm, showed very good correlation with experimental data (Fig. 10).

The results of the simulation are quite similar to the experimental data. Especially at the beginning, about first 100 second of the process, the curves are almost identical.

During computations the end of nucleation is calculated. After this temperature no more grains appears in the melt. This feature of presented model makes it possible to predict the grain density after solidification. In the presented case measured grain density $N_V = 1.4 \cdot 10^{11}$ m^{-3}, and simulated grain density was $1.8 \cdot 10^{11}$ m^{-3}. Both values are at the same order of magnitude.

The grain density growth in time can be observed in the Figure 11. It can be seen that the nucleation phenomenon go on about 10 s. Another interesting thing is that at the end of the nucleation its rate getting smaller, the curve smoothly changes in horizontal line that represents the maximal grain density. In the Figure 12, the grain density growth with temperature decreasing can be observed. In this picture it can be seen that the grain density grows linearly in the center of the temperature domain.

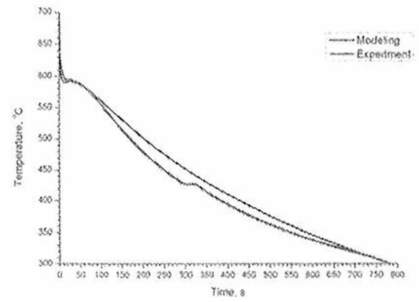

Fig. 10. Cooling curves obtain from simulation and experiment
Rys. 10. Krzywe stygnięcia otrzymane w wyniku symulacji i eksperymentu

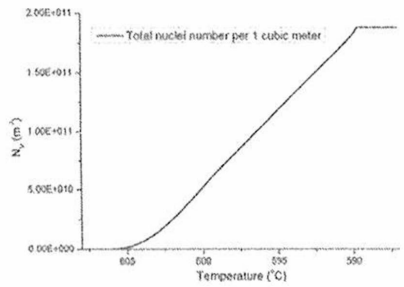

Fig. 12. Grain density versus actual alloy temperature
Rys.12. Zmiana gęstości ziaren w funkcji temperatury stopu

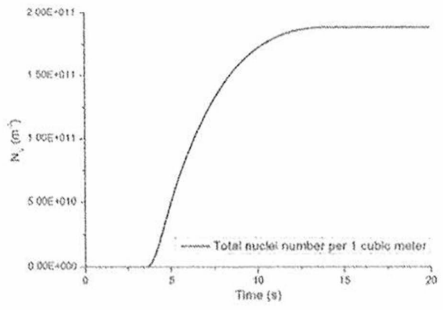

Fig. 11. Kinetic of primary phase nucleation
Rys. 11. Kinetyka zarodkowania fazy pierwotnej

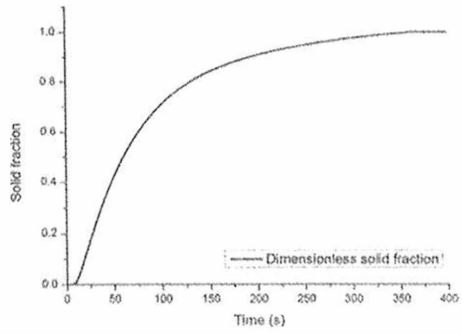

Fig. 13. Kinetic of primary phase solidification
Rys. 13. Kinetyka krzepnięcia fazy pierwotnej

At the time of simulation the volume increments are calculated. Summation of those increments give the actual solidified volume. Actual solidified volume divided by total element volume gives the solid fraction value. The kinetic of solid fraction growth is presented in Figure 13. During the first 100 s of crystallization solid fraction growth faster and after this time the kinetic slows.

CONCLUSIONS

The experimental data can be used to prepare micro-macro composite crystallization model. The model fits good with an experiment results. The differences are probably connected with the assumptions that were made during model preparation and with the fact, that simulation was performed just for one element of the composite.

Numerical simulation gives a lot of useful data that can give new view on the nucleation and solid fraction growth phenomenon. This knowledge can be later used to influence those processes.

The AZ91/SiC nucleation parameters as T_N and N_ν can be described with mathematical formulas. Unknown adjustment parameters can be found using experimental data and statistical algorithms.

The mean volumetric grain density function shows grain density dependence on composite actual undercooling and mass fraction of SiC particles. This knowledge can be very useful for technologists during composite casting procedure preparation.

After setting the mass fraction of SiC particles and derivation the average volumetric grain density function gives information about nucleation rate. This is the key parameter for AZ91/SiC composite micro-macro model of crystallization.

ACKNOWLEDGEMENTS

The authors acknowledge The European Community for financial support under Marie Curie Transfer of Knowledge grant No. MTKD-CT-2006-042468 (AGH No. 27.27.170.304) and Polish Ministry of Science and Higher Education for financial support under grant No. N507-44-66-34 (AGH No. 18.18.170.325).

REFERENCES

[1] Asthana R.: Solidification processing of reinforced metals. Key Engineering Materials 151-152 (1998) 234-300.
[2] Luo A.: Heterogeneous nucleation and grain refinenent in cast Mg(AZ91)/SiC metal matrix composites. Canadian Metallurgical Quaretly 35 (1996) 375-383.
[3] Lelito J., Zak P., Suchy J. S.: The grain nucleation rate of AZ91/SiC composite based on Maxwell-Hellawell model. Archives of Metallurgy and Materials 54 (2009) 347-350.
[4] Fras E., Wiencek K., Gorny M., Lopez H.: Theoretical model for heterogeneous nucleation of grains during nucleation. Material Science and Technology 19 (2003) 1653-59.
[5] Maltais A., Dube D., Fiset M., Laroche G., Tugeon S.: Improvements in the metallography of as-cast AZ91 alloy. Materials Characterization 52 (2004) 103-119.
[6] Maltais A., Dube D., Roy F., Fiset M.: Optical anisotropy of a color-etched AZ91 magnesium alloy. Materials Characterisation 54 (2005) 315-326.
[7] Zak P., Lelito J., Shumcher P., Haberl K., Krajewski W., Suchy J. S.: Color etching of AZ91/SiC composite. XXXIII Konferencja naukowa z okazji Święta Odlewnika, Kraków, Poland 11 grudnia 2009. http://www.odlew.agh.edu.pl/inne/konferencje/dzien_odlewnika_2009.html.
[8] Kapturkiewicz W., Fras E., Burbelko A.: Computer simulation of the austenitizing process in cast iron with pearlitic matrix. Materials Science and Engineering A 413-414 (2005) 352-357.
[9] Johnson W. C., Heckel R. W.: Mathematical modeling of diffusion during multiphase layer growth. Metallurgical Transactions 12 (1981) 1693-97.
[10] Cybo J., Jura S.: Funkcyjny opis struktur izometrycznych w metalografii ilościowej [in Polish]. Wydawnictwo Politechniki Śląskiej, Gliwice, Poland (1995).
[11] Maxwell I., Hellawell A.: A simple model for refinement during solidification. Acta Metallurgica 23 (1975) 229-237.
[12] Quested T. E., Dinsdale A. T., Greer A. L.: Thermodynamic modelling of growth-restriction effects in aluminium alloys. Acta Materialia 53 (2005), 1323-1334.
[13] Kurz W., Fisher D. J.: Fundamentals of solidification. Trans Tech Publications, Zurich (1992).